SCIENCE CHINA
Information Sciences

• RESEARCH PAPER •

August 2020, Vol. 63 180303:1–180303:11
https://doi.org/10.1007/s11432-020-2937-y

Special Focus on mmWave and Terahertz Wireless Communications for B5G/6G

Multitask deep learning-based multiuser hybrid beamforming for mm-wave orthogonal frequency division multiple access systems

Jing JIANG[1*], Yue LI[1], Long CHEN[1], Jianbo DU[1] & Chunguo LI[2]

[1]*School of Information and Communication Engineering, Xi'an University of Posts and Telecommunications, Xi'an 710100, China;*
[2]*School of Information Science and Engineering, Southeast University, Nanjing 210096, China*

Received 2 January 2020/Revised 23 March 2020/Accepted 3 June 2020/Published online 15 July 2020

Abstract Multiuser hybrid beamforming of a wideband millimeter-wave (mm-wave) system is a complex combinatorial optimization problem. It not only needs large training data, but also tends to overfit and incur long run-time when multiple serial deep learning network models are used to solve this problem directly. Preferably, multitask deep learning (MTDL) model could jointly learn multiple related tasks and share their knowledge among the tasks, and this has been demonstrated to improve performance, compared to learning the tasks individually. Therefore, this work presents a first attempt to exploit MTDL for multiuser hybrid beamforming for mm-wave massive multiple-input multiple-output orthogonal frequency division multiple access systems. The MTDL model includes a multitask network architecture, which consists of two tasks-user scheduling and multiuser analog beamforming. First, we use the effective channel with a low dimension as input data for the two parallel tasks to reduce the computational complexity of deep neural networks. In a shallow shared layer of the MTDL model, we utilize hard parameter sharing in which the knowledge of multiuser analog beamforming task is shared with the user scheduling task to mitigate multiuser interference. Second, in the training process of the MTDL model, we use the exhaustive search algorithm to generate training data to ensure optimal performance. Finally, we choose the weight coefficient of each task by traversing all weight coefficient combinations in the training phase. Simulation results prove that our proposed MTDL-based multiuser hybrid beamforming scheme could achieve better performance than traditional algorithms and multiple serial single tasks deep learning scheme.

Keywords millimeter wave systems, user scheduling, deep neural network, multitask learning, hybrid beamforming

Citation Jiang J, Li Y, Chen L, et al. Multitask deep learning-based multi-user hybrid beamforming for mm-wave orthogonal frequency division multiple access systems. Sci China Inf Sci, 2020, 63(8): 180303, https://doi.org/10.1007/s11432-020-2937-y

1 Introduction

In the recent years, millimeter-wave (mm-wave) massive multiple-input multiple-output (MIMO) communication system has become a key enabler for the fifth-generation (5G) mobile communication systems, which leverages large-scale antenna arrays and abundantly available spectrum resources to provide high data rates [1–4]. Moreover, the wideband channel of an mm-wave communication system is frequency selection, so orthogonal frequency division multiple access (OFDMA) could improve the system performance by serving more users and fully achieving multiuser diversity in the entire frequency band. This

* Corresponding author (email: jiangjing@xupt.edu.cn)

means that OFDMA-based frequency resource allocation can effectively improve the spectral efficiency of mm-wave massive MIMO communication systems. However, for a hybrid beamforming architecture of mm-wave massive MIMO systems, analog beamforming is implemented by the phase shifts, which are the same in the entire frequency band [5]. In other words, users in a frequency-multiplexed wideband will experience the same analog beamforming. The multiuser hybrid beamforming for an mm-wave OFDMA system comprises of both user scheduling and analog beamforming, which are coupled together. To acquire the global optimal solution, it is essential to jointly optimize OFDMA user scheduling and analog beamforming in mm-wave massive MIMO OFDMA Systems.

The joint optimization of user scheduling and analog beamforming has attracted widespread attention [6–9]. It was formulated as a nonconvex and combinatorial optimization problem, where the base station (BS) selects a subset of users and their analog beam to multiplex in a beam domain based on the signal-to interference plus noise ratio (SINR) feedback in [6], the limited effective channel state information (CSI) in [7], and the statistical (CSI) in [8], respectively. In [9], it was decoupled into three sub-problems, including OFDMA user grouping, resources allocation and multi-user hybrid beamforming; and, they were solved sequentially. In the above-stated studies, solutions to the joint optimization problem are about mutual coupling and lead to high computational complexity. Moreover, an improved algorithm with low complexity would compensate for the obvious performance loss, since the global optimum is not obtained, due to the limited number of iterations.

Machine learning (ML) techniques have recently performed extraordinarily in processing big data and solving complex combinatorial optimization problems [10]. Thus, we tend to exploit the high-performance of ML techniques to solve the joint optimization problem of user scheduling and analog beamforming. For deep learning with multiple tasks, the authors in [11] proposed an comprising of two modules, namely, the feature extraction module and the feature compression module, which are achieved sequentially by a convolutional neural network and a fully-connected neural network (NN), respectively. In [12], the original iterative structure for turbo decoding was replaced by multiple serial deep neural network (DNN) decoding unit and each achieved a decoding iteration. However, multiple serial DNNs do not only need large amounts of training data, but also can easily lead to overfitting and longer training latency.

Inspired by human learning activities, where people often apply the knowledge they have learned from previous tasks to help them learn a new task, multitask learning (MTL) learns multiple related tasks in parallel and shares the learned knowledge among the multiple tasks. Moreover, this learning method has demonstrated promising performance gains in many applications, e.g., speech recognition [13], computer vision [14], and pattern recognition [15]. Therefore, we propose a multitask deep learning (MTDL) model for the joint optimization of user scheduling and multiuser hybrid beamforming. The contributions of this work are summarized as follows:

(1) The proposed MTDL model consists of two tasks- user scheduling and multiuser analog beamforming. We used an effective channel with a low dimension as input data for the two parallel tasks, which can greatly reduce the computational complexity in training DNNs. In a lower shared layer of the MTDL model, we utilize hard parameter sharing to improve the generalization and speedup the learning rate of the model. In detail, we employed the knowledge obtained from the multiuser analog beamforming task in the user scheduling task to mitigate multiuser interference. In an upper layer of the MTDL model, each task is optimized in a task-specific layer to reinforce the learning effects of the specific task.

(2) For training the MTDL model, we employed an exhaustive search algorithm to generate training data with optimal performance. To improve generalization and speedup the learning rate, we adopted a joint training, where MTDL parameters are adjusted to minimize the joint loss which represents the weighted loss sum of user scheduling task and multi-user analog beamforming task. Furthermore, we set the weight coefficient of each task by traversing all weight coefficient combinations when training the model to minimize the loss function.

(3) Simulation results validate that our proposed MTDL scheme could achieve better performance than traditional algorithms and multiple serial deep learning (DL) tasks. Moreover, compared to traditional algorithms, our proposed model achieves a better run-time.

The rest of the work is organized as follows. In Section 2, we built an mm-wave massive multiuser-

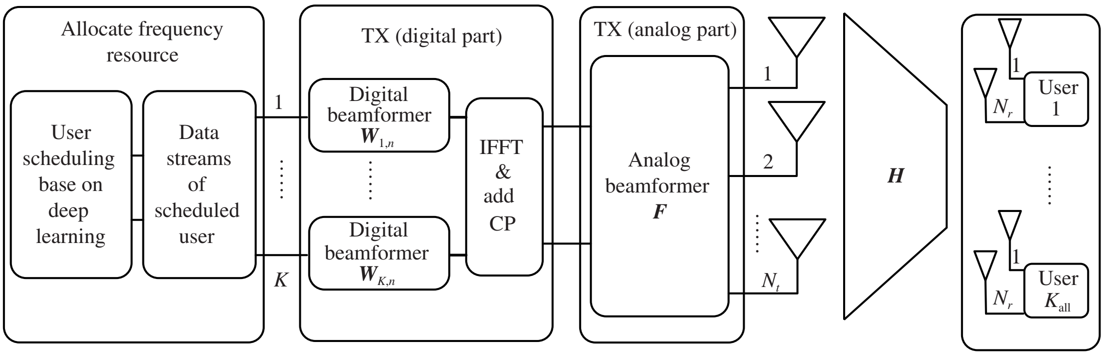

Figure 1 The structure of multi-user hybrid beamforming scheme.

MIMO (MU-MIMO) OFDMA system model and a multi-path wideband channel. Then in Section 3, we discussed the proposed novel MTDL-based multiuser hybrid beamforming for OFDMA Systems. In Section 4, we presented simulation results. Finally, in Section 5, we concluded.

Notations. We denote matrices, vectors, and scalars by bold uppercase letters, bold lowercase letters, and lowercase letters, respectively. Signs $\mathbb{C}^{M\times N}$, $(\cdot)^{\rm H}$, $(\cdot)^{\rm T}$, $\|\cdot\|$ and $\|\cdot\|_{\rm F}$ represent $M\times N$ complex matrix, conjugate transpose, transpose, norm and normalized Frobenius norm, respectively. $\boldsymbol{I}_N$ denotes the $N\times N$ identity matrix. An $M\times N$ all-zero matrix is denoted by $O_{M\times N}$. $\emptyset$ denotes an empty set. $\Re$ and $\Im$ indicate real and imaginary parts of a complex vector, respectively. E represents expectation operator.

2 mm-wave massive MU-MIMO OFDMA system model

2.1 System model

We consider a downlink mm-wave massive MU-MIMO system, as shown in Figure 1, where a BS with $N_{\rm RF}$ radio frequency (RF) chains serves $K_{\rm all}$ users. The BS and each user are equipped with N_t and N_r antennas, respectively. Furthermore, we assumed that the BS sends N_s data streams satisfying $N_s \leqslant N_{\rm RF} \leqslant N_t$. In the entire frequency band, there are $N_{\rm RB}$ resource blocks (RBs) and each RB occupies N_f adjacent subcarriers and N_o consecutive OFDM symbols. During data transmission, a transmitted signal is first processed by baseband digital beamforming, second, an inverse fast Fourier transform is applied to the signal, third, a cyclic prefix is added to the signal, and finally, the signal is sent through RF after being processed by analog beamforming to users in a wireless transmission environment $\boldsymbol{H}$. For the kth user scheduled in the nth RB, the received signal $Y_{k,n}\in\mathbb{C}^{N_s\times 1}$ can be modeled as

$$\boldsymbol{Y}_{k,n}=\boldsymbol{H}_{k,n}\boldsymbol{F}\boldsymbol{W}_{k,n}\boldsymbol{s}_{k,n}+\sum_{\substack{j=1\\ j\neq k}}^{N_{\rm RF}}\boldsymbol{H}_{k,n}\boldsymbol{F}\boldsymbol{W}_{j,n}\boldsymbol{s}_{j,n}+\boldsymbol{n}_{k,n}, \tag{1}$$

where $\boldsymbol{s}_{k,n}\in\mathbb{C}^{N_s\times 1}$ is the transmitted signal vector with $\mathrm{E}[\boldsymbol{s}_{k,n}\boldsymbol{s}_{k,n}^{\rm H}]=\boldsymbol{I}$. $\boldsymbol{W}_{k,n}\in\mathbb{C}^{N_{\rm RF}\times N_s}$ denotes the digital baseband beamformer for the kth user scheduled in the nth RB. $\boldsymbol{F}\in\mathbb{C}^{N_t\times N_{\rm RF}}$ is the analog beamformer and only gets the phase changes with variable phase shifters. $\boldsymbol{F}=[\boldsymbol{f}_1,\boldsymbol{f}_2,\ldots,\boldsymbol{f}_{N_{\rm RF}}]$, where $\boldsymbol{f}_n$ is the analog beam vector of the nth RF chain. In addition, the analog beamformer is implemented through a codebook-based manner and the predefined codebook can be denote as $\mathcal{F}=[\boldsymbol{c}_1,\boldsymbol{c}_2,\ldots,\boldsymbol{c}_{N_c}]$, where N_c is the codebook size. Notably, the total power constraint is enforced by letting $\|\boldsymbol{F}\boldsymbol{W}\|_{\rm F}^2=N_s$. $\boldsymbol{H}_{k,n}\in\mathbb{C}^{N_r\times N_t}$ is the channel matrix from BS to the kth user and $\boldsymbol{n}_{k,n}$ is the additive Gaussian noise with zero-mean and variance σ^2.

2.2 Channel model

For wideband mm-Wave massive MIMO communication systems, the propagation delay of electromagnetic waves traveling across the whole array cannot be ignored. Thus, we consider the beam squint effect in a channel model which makes the array response vary with frequency [16–18]. The uniform linear array consisting of N_t antennas at BS is considered, and the antenna spacing is d. To formulate the channel model, we assume that there are P_k transmission paths between kth user and BS and the time delay of the pth path to the first antenna of the BS is denoted as $\tau_{k,p,1}$. If the angle-of-departure (AoD) of the pth path is $\phi_{k,p}$, and the normalized angle-of-arrival can be represent as $\theta_{k,p} = \frac{d\sin(\phi_{k,p})}{\lambda_c}$, where λ_c is the length of the carrier frequency. Then, the time delay of the pth path to the mth antenna can be denoted as follows:

$$\tau_{k,p,m} = \tau_{k,p,1} + (m-1)\frac{d\sin(\phi_{k,p})}{c}, \tag{2}$$

where c represents the speed of light. According to the relationship between c and carrier frequency f_c, the time delay can be further expressed as

$$\tau_{k,p,m} = \tau_{k,p,1} + (m-1)\frac{\theta_{k,p}}{f_c}. \tag{3}$$

In addition, the channel impulse response from the mth antenna to the kth user can be denoted as

$$h_{k,m}(t) = \sum_{p=1}^{P_k} \beta_{k,p} \mathrm{e}^{-\mathrm{j}2\pi f_c \tau_{k,p,1}} \mathrm{e}^{-\mathrm{j}2\pi(m-1)\theta_{k,p}} \delta(t-\tau_{k,p,m}), \tag{4}$$

where $\beta_{k,p}$ is the complex gain. Considering the Fourier transform of Eq. (4), we obtain frequency-domain representation over all M antennas $\boldsymbol{H}_k(f)$ as follows:

$$\boldsymbol{H}_k(f) = \sum_{p=1}^{P_k} \beta_{k,p} \mathrm{e}^{-\mathrm{j}2\pi f_c \tau_{k,p,1}} \boldsymbol{a}(\theta_{k,p}, f) \mathrm{e}^{-\mathrm{j}2\pi f \tau_{k,p,1}}, \tag{5}$$

where $\boldsymbol{a}(\theta_{k,p}, f)$ is the wideband array steering vector and expressed as

$$\boldsymbol{a}(\theta_{k,p}, f) = \left[1, \ldots, \mathrm{e}^{-\mathrm{j}2\pi(N_t-1)\theta_{k,p}(1+\frac{f}{f_c})}\right]^{\mathrm{T}}. \tag{6}$$

2.3 Problem formulation

The objective of this work is to design the user scheduling and analog beamforming at the BS to maximize the total transmission rate. From (1), the achievable rate of the kth user scheduled in the nth RB can be expressed as

$$R_{k,n} = \log_2(1+\gamma_{k,n}), \tag{7}$$

where the received SINR $\gamma_{k,n}$ is given by

$$\gamma_{k,n} = \frac{\|\boldsymbol{H}_{k,n}\boldsymbol{F}\boldsymbol{W}_{k,n}\boldsymbol{s}_{k,n}\|^2}{\sigma^2 + \sum_{j=1,j\neq k}^{N_{\mathrm{RF}}} \|\boldsymbol{H}_{k,n}\boldsymbol{F}\boldsymbol{W}_{j,n}\boldsymbol{s}_{j,n}\|^2}. \tag{8}$$

Then, the sum-rate of the system can be expressed as

$$R_{\mathrm{sum}}(\mathcal{R}, \mathcal{B}) = \sum_{n=1}^{N_{\mathrm{RB}}} \sum_{k=1}^{N_{\mathrm{RF}}} R_{k,n}, \tag{9}$$

where $\mathcal{R}$ and $\mathcal{B}$ are the results of the user scheduling and the multiuser selection, respectively. However, for the mutual coupling of user scheduling and multiuser hybrid beamforming joint optimization problem, an optimal closed solution cannot be obtained. The user scheduling result is sub-optimal, and it will lead to high computational complexity. The usual solution is by decoupling. Preferably, the powerful computing and cognitive capabilities of DL make it an excellent tool that could effectively obtain an optimal solution for the coupling of user scheduling and multiuser hybrid beamforming joint optimization problem. Since the frequency resources and RF chains are limited in mm-wave OFDMA Systems, the joint optimizing problem can be designed as a classification problem and processed using a supervised DL model. Then, $\mathcal{R}$ and $\mathcal{B}$ are the label data. The element $\mathcal{R}_{k,n} \in \{0,1\}$ means whether or not the nth resource is utilized by the kth user. $\mathcal{B}_{k,n_c} \in \{0,1\}$ and $\mathcal{B}_{k,n_c} = 1$ indicates the kth MU-MIMO user is transmitted by the n_cth analog beam at the BS. The joint optimization problem can be formulated as

$$\begin{aligned} \mathcal{P}_0: \quad & \arg\max_{\mathcal{R},\mathcal{B}} R_{\mathrm{sum}}(\mathcal{R},\mathcal{B}) \\ \text{s.t.} \quad & |\boldsymbol{F}(i,j)| = 1, \ \forall i,j, \\ & \|\boldsymbol{F}\boldsymbol{W}\|_{\mathrm{F}}^2 = N_s, \end{aligned} \tag{10}$$

where each element of $\boldsymbol{F}$ is constant-magnitude entries, satisfies $|\boldsymbol{F}(i,j)| = 1$, $\forall i,j$. The total power constraint of the BS is enforced by normalizing $\boldsymbol{W}$ as $\|\boldsymbol{F}\boldsymbol{W}\|_{\mathrm{F}}^2 = N_s$.

3 MTDL-based joint design scheme

In this section, we will explain the proposed MTDL-based joint design scheme. We design the user scheduling task and multiuser analog beamforming as classification tasks, respectively. Classification categories (labels) are the RB number N_{RB} and the codeword number N_c, respectively. However, training two classification neural networks independently is time-consuming. Further, the user scheduling and multiuser hybrid beamforming are mutually coupled as joint optimization problem, so using two independently trained networks to solve this joint optimization problem is practically inadequate. Following these considerations, we introduce MTL to solve the joint optimization problem and propose the MTDL-based joint design scheme. The MTDL model allows multiple tasks to learn at the same time, which reduces training complexity and greatly reduces time latency [19]. In addition, a shared representation mechanism is introduced into the scheme, which is achieved by sharing hidden layers parameters among all tasks, and allowing tasks to share feature information and thereby, promote learning. Shallow shared representations improve the learning rate of the networks, which enhances the learning effect of each task. In the next subsections, we will describe the proposed scheme and the training strategy in detail. Then, a digital beamforming design based on the predicted results of the MTDL scheme is presented.

3.1 MTDL-based joint optimization scheme

A fully connected structure of the MTDL-based joint optimization scheme is shown in Figure 2. It consists of two tasks: user scheduling and multiuser analog beamforming. The MTDL network includes four layers: an input layer, a shared layer, a task-specific layer, and an output layer.

In this work, input data set is the same for two tasks mentioned above. To reduce the dimension of the input data and the training time significantly, the input tuple is first pre-processed by an initial analog beamformer that is fed back from each user, and then, is normalized by the input layer to improve the stability of the MTDL model. $\boldsymbol{x}_{\mathrm{in}}$ is the input data set and can be described as

$$\boldsymbol{x}_{\mathrm{in}} = \left\{ \hat{\boldsymbol{H}}_1, \hat{\boldsymbol{H}}_2, \ldots, \hat{\boldsymbol{H}}_{K_{\mathrm{all}}}, \boldsymbol{c}_{\boldsymbol{B}_1}, \boldsymbol{c}_{\boldsymbol{B}_2}, \ldots, \boldsymbol{c}_{\boldsymbol{B}_{K_{\mathrm{all}}}} \right\}, \tag{11}$$

where $\boldsymbol{B}_k$ is the index of optimal beam fed back from the kth user. $\hat{\boldsymbol{H}}_k = [\Re(\overline{\boldsymbol{H}}_k), \Im(\overline{\boldsymbol{H}}_k)]$ is the processed effective analog channel matrix of the kth user and $\overline{\boldsymbol{H}}_k = [\overline{\boldsymbol{H}}_{k,1}, \overline{\boldsymbol{H}}_{k,2}, \ldots, \overline{\boldsymbol{H}}_{k,N_{\mathrm{RB}}}]$ is the effective analog channel in the wideband, where $\overline{\boldsymbol{H}}_{k,n}$ is the effective analog channel matrix of the kth user in the nth RB and is given by $\overline{\boldsymbol{H}}_{k,n} = \boldsymbol{H}_{k,n}\boldsymbol{f}_{B_k}$.

Next, we utilize a DNN to learn the nonlinear mapping function between the input tuple and the joint optimization results. The output of the lth layer of the ith task is given by

$$\boldsymbol{x}_{i,l} = \begin{cases} f_R\left(\Theta_{i,l}\boldsymbol{x}_{\mathrm{in}} + b_{i,l}\right), & l = 1, \\ f_R\left(\Theta_{i,l}\boldsymbol{x}_{i,l-1} + b_{i,l}\right), & 1 < l \leqslant L, \end{cases} \tag{12}$$

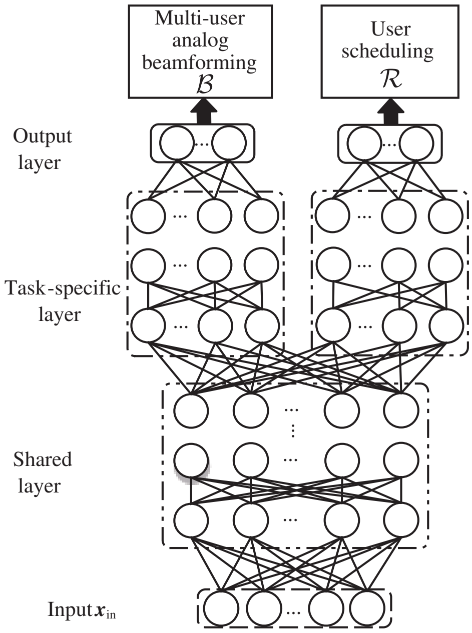

Figure 2 The structure of multitask deep learning-based multiuser hybrid beamforming scheme.

where $\Theta_{i,l}$ and $b_{i,l}$ are the weight and the bias of the lth layer of the ith task, respectively, and L is the total number of hidden layers. To significantly reduce possibility of overfitting, we utilize hard parameter sharing in the shallow shared layer, which can share the important knowledge and achieve a reinforcement among the different tasks [13]. Specifically, the knowledge of multiuser analog beamforming task is shared with the user scheduling task to mitigate the multiuser interference and obtain a higher-sum rate through scheduling decision. Moreover, each task is optimized in the task-specific layer to reinforce learning effects. The rectified linear unit [20] function is introduced to realize non-linearity, which is given by $f_R(z) = \max\{0, z\}$.

Finally, predicted data of the MTDL network is acquired and the results of user scheduling and multiuser analog beamforming are obtained by processing the predicted data. The processing method is described in the section of training strategy of MTDL. The output of the ith task can be expressed as

$$\boldsymbol{o}_i = f_S\left(\Theta_{i,L}\boldsymbol{x}_{i,L} + b_{i,L}\right), \tag{13}$$

which employs sigmoid function to generate probabilities, and the sigmoid function is given by $f_S(z) = \frac{1}{1+\mathrm{e}^{-z}}$. Moreover, due to a large number of parameters, the MTDL model may tend to overfit. We used the dropout technique to prevent possible overfitting. The key idea is to randomly drop units and their connections from NN during training which prevents network units from co-adapting too much. In the MTDL model, we set the dropout rate to 0.5, which is close to the optimal rate for a wide range of networks and tasks [21].

3.2 Network training

3.2.1 *Training data set generation*

In this stage, we adopt an offline learning scheme to train the MTDL model. To generate the training data, we assume that the perfect CSI is only available to compute output labels. Specifically, we generate the labeled data, i.e., $\mathcal{R}$ and $\mathcal{B}$, which are the optimal scheme of the user scheduling and the multiuser selection, respectively. The specific generation process is shown in Algorithm 1 based on the exhaustive search algorithm. In addition, since the NN requires its input data to be real values, we represent user CSI by real and imaginary components. Therefore, the input data can be given by $\boldsymbol{x}_{\text{in}} = \{\hat{\boldsymbol{H}}_1, \hat{\boldsymbol{H}}_2, \ldots, \hat{\boldsymbol{H}}_{K_{\text{all}}}, \boldsymbol{c}_{\boldsymbol{B}_1}, \boldsymbol{c}_{\boldsymbol{B}_2}, \ldots, \boldsymbol{c}_{\boldsymbol{B}_{K_{\text{all}}}}\}$, where $\hat{\boldsymbol{H}}_k = [\Re(\overline{\boldsymbol{H}}_k), \Im(\overline{\boldsymbol{H}}_k)]$ and training sample can be represented as $\{\boldsymbol{x}_{\rm in}, \mathcal{R}, \mathcal{B}\}$. By repeating the above process for multiple number of times, the entire training data set can be obtained. The test data set is also generated in the same way.

Algorithm 1 Generation of the training data

Input: $\boldsymbol{x}_{\rm in}$.
Output: $\mathcal{R}$, $\mathcal{B}$.
Initialization: $\mathcal{M} \in O(K_{\rm all} \times N_c)$, $\mathcal{U} \in O(N_c \times N_{\rm RB})$, $\mathcal{R} \in O(K_{\rm all} \times N_{\rm RB})$, $\mathcal{B} \in O(K_{\rm all} \times N_c)$, the selected MU-MIMO user set $\Omega_S = \emptyset$.

1: According to the best beam index of each user, set the corresponding element of $\mathcal{M}$ to 1, e.g., if $\boldsymbol{B}_k = n_c$, then $\mathcal{M}(k, n_c) = 1$.

2: Assume there are Q_{n_c} possible schemes of resource allocation for users with the same best beam. Exploiting the exhaustive search algorithm to find the user scheduling scheme with the maximum sum rate.

  for $n_c = 1 : N_c$
    for $q = 1 : Q_{n_c}$
      $\{k^*\} = \arg\max_q \sum_{n=1}^{N_{\rm RB}} \left(\frac{\|\overline{\boldsymbol{H}}_{k,n}\|^2}{\sigma^2} \right)$,
      $\mathcal{U}(n_c, n) = k^*$ and $\mathcal{R}(n_c, n) = 1$,
    end
  end

3: After resource allocation, each beam is regarded as a virtual OFDMA user multiplexing the whole frequency resource. Then, the integrated channel of each virtual OFDMA user is merged as follows, $\Omega = \{\tilde{\boldsymbol{H}}_{n_1}, \tilde{\boldsymbol{H}}_{n_2}, \ldots, \tilde{\boldsymbol{H}}_{N_c}\}$ and $\tilde{\boldsymbol{H}}_{n_c} = [\boldsymbol{H}_{\mathcal{U}(n_c,1)} | \boldsymbol{H}_{\mathcal{U}(n_c,2)} | \cdots | \boldsymbol{H}_{\mathcal{U}(n_c,N_{\rm RB})}]_{N_r \times N_t}$ is the channel matrix of a user allocated in the nth RB for the n_cth virtual OFDMA user. When a frequency resource is not been allocated to any user, $\boldsymbol{H}_{\mathcal{U}(n_c,n)}$ is equal to zero matrix.

4: Select $N_{\rm RF}$ virtual OFDMA users to maximizes sum-rate.

  for $n_c = 1 : N_{\rm RF}$
    if $n_c = \max_{\tilde{H}_{n_c} \in \Omega} \log_2 \Big(1 + \frac{\|\boldsymbol{U}_{n_c}^{\rm H} \tilde{\boldsymbol{H}}_{n_c} \boldsymbol{V}_{n_c}\|^2}{\delta^2 + \sum_{j \in \Omega_s, n_c \in \Omega} \|\boldsymbol{U}_j^{\rm H} \tilde{\boldsymbol{H}}_{n_c} \boldsymbol{V}_j\|^2} + \sum_{j \in \Omega_s} \frac{\|\boldsymbol{U}_j^{\rm H} \tilde{\boldsymbol{H}}_j \boldsymbol{V}_j\|^2}{\delta^2 + \|\boldsymbol{U}_{n_c}^{\rm H} \tilde{\boldsymbol{H}}_j \boldsymbol{V}_{n_c}\|^2 + \sum_{i \in \Omega_s, i \neq j} \|\boldsymbol{U}_i^{\rm H} \tilde{\boldsymbol{H}}_j \boldsymbol{V}_i\|^2} \Big)$,
    where $\boldsymbol{U}$ and $\boldsymbol{V}$ are the left unitary matrix and the right unitary matrix of the singular value decomposition of virtual OFDMA user $\tilde{\boldsymbol{H}}_{n_c}$, respectively.
    then $\mathcal{B}(:, n_c) = 1$, $\Omega \leftarrow \Omega \backslash \{\tilde{\boldsymbol{H}}_{n_c}\}$, $\Omega_s \leftarrow \Omega_s \cup \{\tilde{\boldsymbol{H}}_{n_c}\}$.
  end

3.2.2 *Training strategy of MTDL*

To improve generalization and speed up the learning rate, the joint training mode is adopted where MTDL parameters are adjusted to minimize the joint loss function. Specifically, the joint loss function is optimized in the MTDL model and is defined as

$$\text{Loss}_{\text{joint}} = \sum_{i=1}^{2} \lambda_i \text{Loss}_i, \tag{14}$$

where Loss_i is the loss function of the ith task. λ_i is the weight coefficient and adjusted by traversing all weight coefficient combinations in the training phase to minimize the joint loss function. Results demonstrate that the loss function is smallest when the weight coefficients are all 1. For each task, the cross entropy loss function is formulated as

$$\text{Loss}_i = -\sum [l_i \ln \boldsymbol{o}_i + (1 - l_i) \ln(1 - \boldsymbol{o}_i)], \tag{15}$$

where l_i is the labeled data of the ith task. During the training process, the model parameters are updated by the Adam optimizer [22] to minimize the joint loss function continuously, which not only calculates the adaptive parameter learning rate based on the first-order moment (mean), but also makes full use of the second-order moment (variance) of the gradient, so that optimization efficiency can be guaranteed.

Finally the selected OFDMA user and the user scheduling are obtained from the predicted data. Specifically, it is described as follows:

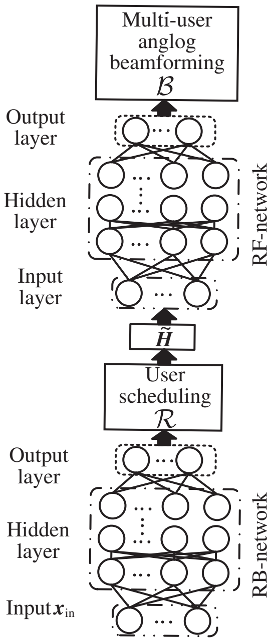

Figure 3 The structure of single task deep learning-based multiuser hybrid beamforming scheme.

Step 1. Predicted probabilities for the multiuser analog beamforming task are sorted in descending order. The virtual OFDMA user corresponding to the top N_{RF} values are chose as the multiplexing analog beams which can be expressed as $\boldsymbol{F} = [\boldsymbol{f}_1, \boldsymbol{f}_2, \ldots, \boldsymbol{f}_{N_{\mathrm{RF}}}]$.

Step 2. For the first selected analog beam, the user with the maximum probability is scheduled in the corresponding RB according to the predicted probabilities for the user scheduling task. Repeat the resource allocation process for each analog beam, and all RB can be allocated to multiple MU-MIMO users.

3.3 Digital beamforming design

Based on the analog beamformer and the user scheduling results, the digital beamformer $\boldsymbol{W}$ is designed by the zero-forcing algorithm. The digital beamformer in the nth RB can be designed as

$$\boldsymbol{W}_n = (\bar{\boldsymbol{H}}_n^{\mathrm{H}} \bar{\boldsymbol{H}}_n)^{-1} \bar{\boldsymbol{H}}_n^{\mathrm{H}}, \tag{16}$$

where $\bar{\boldsymbol{H}}_n = [\bar{\boldsymbol{H}}^{\mathrm{H}}_{\overline{\mathcal{R}}(1,n)}, \ldots, \bar{\boldsymbol{H}}^{\mathrm{H}}_{\overline{\mathcal{R}}(N_{\mathrm{RF}},n)}]^{\mathrm{H}}$ is the analog effective channel of the nth RB, and $\overline{\mathcal{R}}(:,n)$ is index of the user scheduled in the nth RB. Furthermore, $\boldsymbol{W}_n = [\boldsymbol{W}_{\overline{\mathcal{R}}(1,n),n}, \ldots, \boldsymbol{W}_{\overline{\mathcal{R}}(N_{\mathrm{RF}},n),n}]$, where $\boldsymbol{W}_{\overline{\mathcal{R}}(1,n)}$ is the digital beamformer of the user $\overline{\mathcal{R}}(1,n)$ scheduled in the nth RB.

4 Simulation results and discussions

In this section, we present simulation results of our scheme and compare it with the traditional scheme proposed in [9], the single task deep learning (STDL) scheme and the exhaustion search scheme. For each channel matrix realization, the propagation environment is modeled as $P_k = 5$ paths. The angle of ϕ is uniformly distributed over $[0, \pi]$ and the constant angular spread of AoD is 5°. The predesigned codebook $\mathcal{F}$ is the discrete Fourier transform codebook. The description of the STDL scheme, traditional scheme and exhaustion search scheme are as follows:

(1) The STDL scheme. As shown in Figure 3, the STDL scheme consists of two fully connected networks: RB-Network and RF-Network, which correspond to user scheduling and multiuser analog beamforming respectively. In addition the number of neurons in the hidden layer structure is the same for the two networks, which are 128, 64, and 32, respectively. During the training phase, the networks

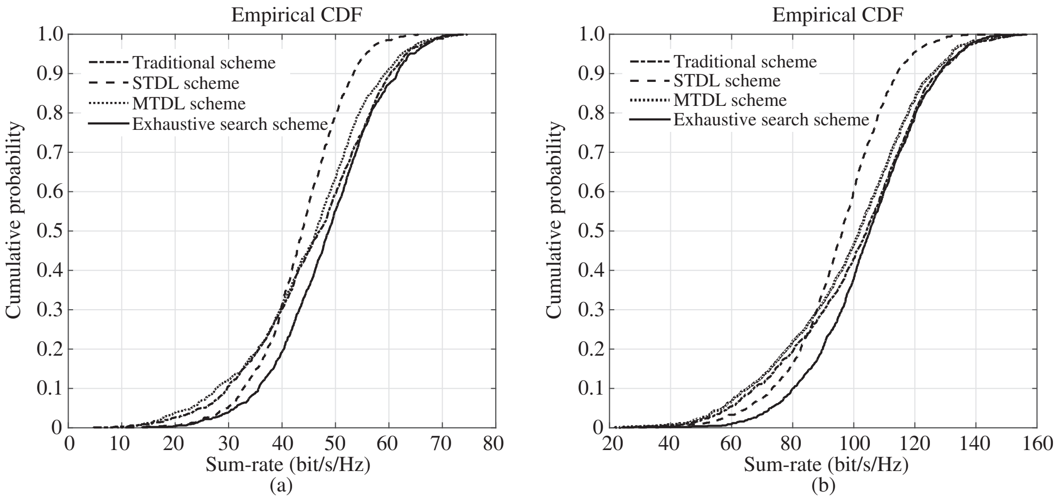

Figure 4 The sum-rate cumulative distribution function (CDF) of different schemes with SNR = 0 dB. (a) $N_{\rm RF} = 2$, $N_{\rm RB} = 2$; (b) $N_{\rm RF} = 2$, $N_{\rm RB} = 4$.

use cross-entropy as the loss function and are optimized by the Adam optimizer. For the RB-Network and RF-Network, the training learning rate is set to 0.001 with a batch size of 100. After training the two networks, the networks work in a cascaded manner. Specifically, the RB-Network first predicts the probability of each user using each RB. According to the probability and the optimal beam index of each other, the integrated channel of each OFDMA group can be obtained. Then, the integrated channels are used as input data for the RF-Network and output data of the RF-Network is the MU-MIMO user selection result. Compared with the MTDL scheme, the STDL is different because the two-task networks are trained independently and there is no knowledge sharing between the tasks (networks).

(2) The traditional scheme. In this scheme, first, the OFDMA user group for users with an identical RF beam is defined. Second, a frequency resource is allocated to each member according to the channel gain, and each OFDMA group is defined as a virtual MU-MIMO user. Then, several MU-MIMO users are selected to maximize the mm-wave system throughput.

(3) The exhaustive search scheme. In the exhaustive search scheme, first, we iterate over combinations of arbitrary $N_{\rm RB}$ users with the same best analog beam and consider the combination with the maximum sum-rate as the result of the OFDMA user scheduling. Second, iteratively compute the sum-rate of the combinations of arbitrary $N_{\rm RF}$ OFDMA visual group, and the combination with the highest sum-rate is selected as the final multiuser analog beamforming result.

For appropriate comparison, the different schemes are implemented with Keras 2.2.4 in Python 3.6.0. For MTDL DNNs, the neuron numbers of the three shared hidden layers from top to bottom are 256, 128, and 64, respectively. The hidden layer in each subnetwork contains 32 nodes. Furthermore, the training learning rate is set to 0.001 with a batch size of 100. The training and test sets consist of 100000 and 1000 samples, respectively, and the validation split is 0.1.

4.1 Network performance evaluation

In this experiment, the sum-rate of our MTDL scheme is evaluated and compared with the STDL scheme, the traditional scheme proposed in [9] and the exhaustion scheme. Figure 4 shows the cumulative distribution function of the sum-rate and the curve counts system sum-rate of 1000 test samples. It is observed that the system sum-rate performance of different schemes increases as the number of RB increases. The sum-rate performance of the exhaustive search scheme is optimal, while the STDL scheme is worst. For the traditional scheme, the sum-rate performance of 50%−70% of samples is inferior to the exhaustive search scheme. The performance of the MTDL scheme is very close to that of the traditional scheme.

Further, we compared the sum-rate to signal-to-noise ratio (SNR). As shown in Figure 5, the sum-rate curve versus the SNR is presented for $N_{\rm RB} = 2$ (Figure 5(a)) and $N_{\rm RB} = 4$ (Figure 5(b)). It is seen that

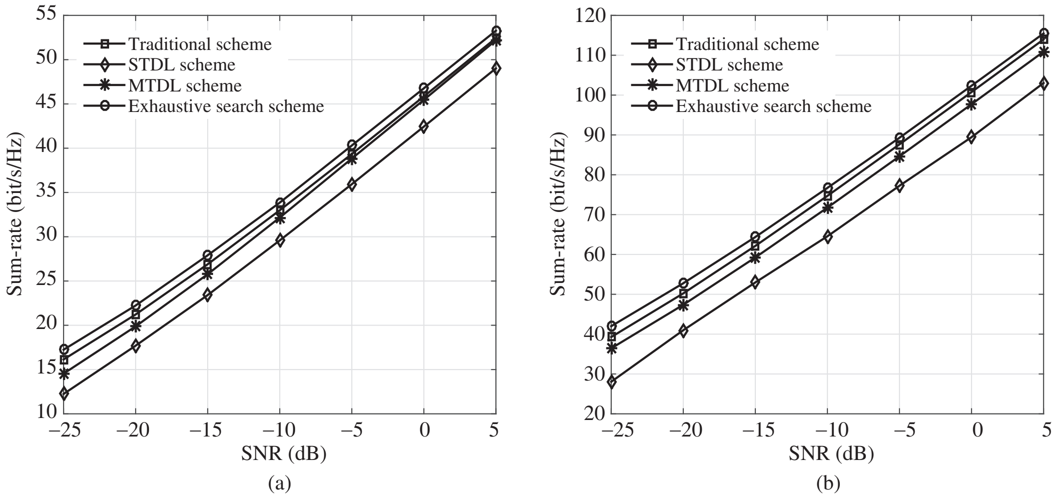

Figure 5 The sum-rate of different scheme versus SNR. (a) $N_{\rm RF}=2$, $N_{\rm RB}=2$; (b) $N_{\rm RF}=2$, $N_{\rm RB}=4$.

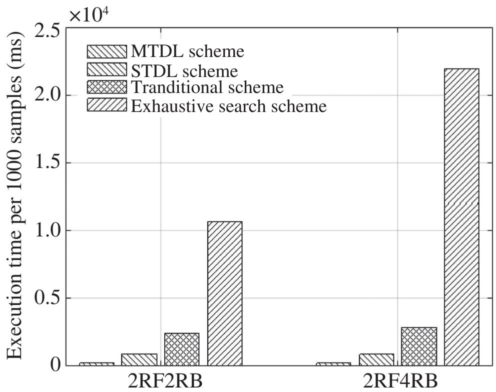

Figure 6 The elapsed time of different schemes.

the performance of the exhaustive search scheme has a smaller advantage over the MTDL scheme and the traditional scheme. The MTDL scheme has a performance gap compared with the traditional scheme in low SNR regimes, and the performance gap decreases as the SNR increases. In the meantime, the performances of these three schemes significantly outperform the STDL scheme. Therefore, the proposed MTDL scheme can effectively approximate the nonlinear mapping relationship between the pre-processed CSI and the joint optimization results.

4.2 Computational evaluation

In this subsection, we evaluate the computational complexity of our proposed scheme, including the run-time from the point where data is inputted into the networks to the point when the joint design results are obtained. The results are shown in Figure 6. As can be seen, the computational complexity of the MTDL scheme is significantly lower than that of the STDL-based scheme, the traditional scheme, and the exhaustive search scheme. This is because a well-trained MTDL network only needs finite steps to obtain scheduling results, while a traditional scheme needs to iterate indefinite times to obtain scheduling results. The exhaustive search scheme needs to traverse and calculate every possible scheduling result, so its computational complexity is the highest. In addition, since the MTDL scheme adopted the MTL mechanism and the shallow shared representations, which improve the learning rate effectively, it is run-time is smaller than that of the STDL scheme. Furthermore, the run-time of the traditional algorithm increases with $N_{\rm RB}$, while that of our proposed scheme almost remains unchanged. These observations indicate that our proposed MTDL scheme can effectively fit a complex algorithm and can be used in real-time with negligible latency.

5 Conclusion

In this work, we proposed an MTDL-based multiuser hybrid beamforming algorithm of mm-wave massive MIMO OFDMA systems. To improve the generalization and speed up the learning rate, the DNNs for the two tasks-user scheduling and multiuser analog beamforming-learn in parallel and share the relative information contained in the shallow shared layer. Specifically, we utilize hard parameter sharing to share the relative knowledge of two coupled tasks, which can mitigate the multiuser interference and obtain more performance gains of user scheduling. Furthermore, we adopt an effective channel with a low dimension as the input data to reduce the computational complexity of DNNs. Simulation results reveal that the MTDL scheme can achieve an equivalent sum-rate performance with a lower run-time than traditional algorithm, and much better than multiple serial single task DLs.

Acknowledgements This work was supported by National Natural Science Foundation of China (Grant Nos. 61871321, 61901367), National Science and Technology Major Project (Grant No. 2017ZX03001012-005), and Shaanxi STA International Cooperation and Exchanges Project (Grant No. 2017KW-011).

References

1 Roh W, Seol J Y, Park J, et al. Millimeter-wave beamforming as an enabling technology for 5G cellular communications: theoretical feasibility and prototype results. IEEE Commun Mag, 2014, 52: 106–113
2 Bogale T E, Le L B. Massive MIMO and mmWave for 5G wireless HetNet: potential benefits and challenges. IEEE Veh Technol Mag, 2016, 11: 64–75
3 Ayach O E, Rajagopal S, Abu-Surra S, et al. Spatially sparse precoding in millimeter wave MIMO systems. IEEE Trans Wirel Commun, 2014, 13: 1499–1513
4 Sharma S K, Bogale T E, Le L B, et al. Dynamic spectrum sharing in 5G wireless networks with full-duplex technology: recent advances and research challenges. IEEE Commun Surv Tut, 2018, 20: 674–707
5 Samimi M K, Rappaport T S. Ultra-wideband statistical channel model for non line of sight millimeter-wave urban channels. In: Proceedings of IEEE Global Communications Conference (GLOBECOM), 2014. 3483–3489
6 Kwon G, Park H. A joint scheduling and millimeter wave hybrid beamforming system with partial side information. In: Proceedings of IEEE International Conference on Communications (ICC), 2016
7 He S W, Wu Y P, Ng D W K, et al. Joint optimization of analog beam and user scheduling for millimeter wave communications. IEEE Commun Lett, 2017, 21: 2638–2641
8 Jiang Z Y, Chen S, Zhou S, et al. Joint user scheduling and beam selection optimization for beam-based massive MIMO downlinks. IEEE Trans Wirel Commun, 2018, 17: 2190–2204
9 Jiang J, Kong D T. Joint user scheduling and MU-MIMO hybrid beamforming algorithm for mmWave FDMA massive MIMO system. Int J Antenna Propag, 2016, 2016: 1–10
10 Qin Z J, Ye H, Li G Y, et al. Deep learning in physical layer communications. IEEE Wirel Commun, 2019, 26: 93–99
11 Lu C, Xu W, Shen H, et al. MIMO channel information feedback using deep recurrent network. IEEE Commun Lett, 2019, 23: 188–191
12 He Y F, Zhang J, Wen C K, et al. TurboNet: a model-driven DNN decoder based on max-log-map algorithm for turbo code. 2019. ArXiv:1905.10502
13 Ruder S. An overview of multi-task learning in deep neural networks. 2017. ArXiv:1706.05098
14 Sun Y, Wang X G, Tang X O. Deep learning face representation by joint identification-verification. 2014. ArXiv:1406.4773
15 Alkhateeb A, El Ayach O, Leus G, et al. Channel estimation and hybrid precoding for millimeter wave cellular systems. IEEE J Sel Top Signal Process, 2014, 8: 831–846
16 Cai M M, Gao K, Nie D, et al. Effect of wideband beam squint on codebook design in phased-array wireless systems. In: Proceedings of IEEE Global Communications Conference (GLOBECOM), 2016
17 Wang B L, Jian M N, Gao F F, et al. Beam squint and channel estimation for wideband mmwave massive MIMO-OFDM systems. IEEE Trans Signal Process, 2019, 67: 5893–5908
18 Wang M J, Gao F F, Shlezinger N, et al. A block sparsity based estimator for mmwave massive MIMO channels with beam squint. IEEE Trans Signal Process, 2020, 68: 49–64
19 Caruana R. Multitask learning. Mach Learn, 1997, 28: 41–75
20 Nair V, Hinton G E. Rectified linear units improve restricted boltzmann machines. In: Proceedings of the 27th International Conference on Machine Learning (ICML-10), 2010. 807–814
21 Srivastava N, Hinton G F, Krizhevsky A, et al. Dropout: a simple way to prevent neural networks from overfitting. J Mach Learn Res, 2014, 15: 1532–4435
22 Kingma D, Ba J. Adam: a method for stochastic optimization. In: Proceedings of the 3rd International Conference on Learning Representations (ICLR), 2014